DESIGNING A COMPACT RIDGED WAVEGUIDE FILTER WITH CST FILTER DESIGNER 3D

WHITEPAPER

Multi-mode cavity filters offer high power handling and good performance as a compact device. Such filters are complex and sensitive to changes in the structure, meaning that their design can be time-consuming or even impossible with conventional methods. This article shows how the CST Studio Suite® filter synthesis tool can be used to design and tune a multi-mode compact ridged waveguide filter to meet stringent specifications.

The proliferation of mobile communication systems and protocols means frequency spectrum utilization is increasingly restricted – realizing the stringent channel specifications requires high-performance band-pass filters. Satellite systems in particular are very exact in frequency, power, size and weight requirements: the filter response should produce a steep cut-off to avoid channel interference and to adhere to various standards, but size and space are typically restricted. Cavity filters are typically the preferred choice due to their power handling capabilities, but they are often bulky and heavy. Multi-mode cavity filters are therefore an attractive alternative. They use a number of modes in a single cavity, which significantly reduces the overall size[1]. They also allow cross-couplings between cavities for a better filter response, which is not always possible for single mode resonators due to physical restrictions.

There are several simulation techniques that can be used in the tuning process of coupled-resonator filters[2]. One traditional approach is to sequentially build up the filter by adding only one resonator at a time, while the group delay of the reflected signal is used as the figure of merit for the optimization[3]. Another approach is to apply the inverse chirp Z-transformation to the reflected signal and from the transient response identify the individual detuned resonators and couplings[2]. It is also possible to add additional ports to the full-wave simulation model and connect lumped components in a coupled schematic for space mapping[4]. All of these techniques typically involve using an equivalent circuit as a surrogate model where intermediate results can quickly be obtained as a reference during the process.

However, these are not well suited to the design of multimode cavity filters. Often, these approaches are impractical for such a complex filter and, even if they can be applied, the narrow bandwidth makes the structure inherently sensitive to small changes in the geometry.

This whitepaper sets out a different approach, which involves the direct extraction of the coupling matrix using the Filter Designer 3D solver in combination with full-wave 3D simulation in CST Studio Suite. The design workflow presented here is for a dual-mode filter with an unconventional cavity configuration, where square ridge resonators[5] are coupled through broadside irises (see Figure 1). This not only provides good control over the individual coupling coefficients, but it also produces a compact solution for satellite communication systems.

SPECIFICATIONS: FILTER RESPONSE AND TOPOLOGY

For this filter the specified center frequency is 10 GHz, with a passband return loss of more than 20 dB over a 100 MHz bandwidth (equal to 1% fractional bandwidth (FBW)). As the filter needs both high selectivity and a compact design, an 8th-order transfer function is used with two symmetric pairs of transmission zeros centred around the passband. This S-parameter response is illustrated in Figure 2.

From the specified filter response, Filter Designer 3D produces a range of potential filter topologies. The chosen topology for this design, with corresponding coupling matrix shown in Figure 3, consists of two cascaded quadruplet sections which are directly responsible for the two transmission zero pairs.

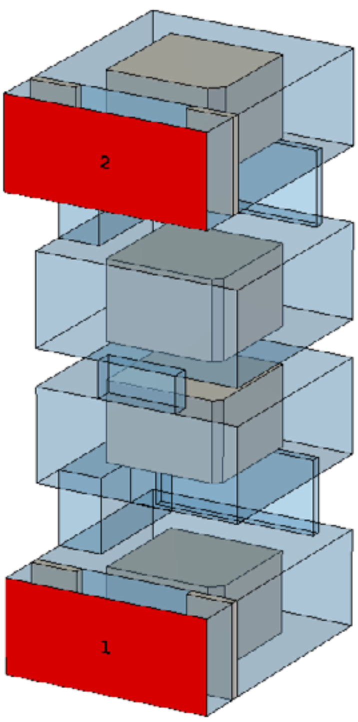

Figure 1: The 8th order ridged waveguide filter model.

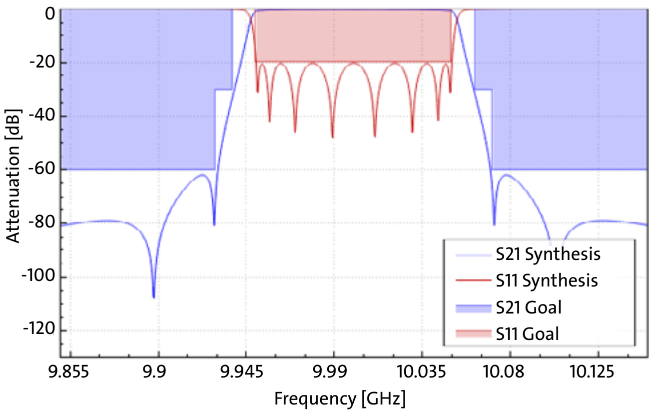

Figure 2: The S-parameters of the synthesized filter response.

	S	1	2	3	4	5	6	7	8	L
S	0	0.9871	0	0	0	0	0	0	0	0
1	0.9871	0	0.7945	0	-0.1855	0	0	0	0	0
2	0	0.7945	0	0.7078	0	0	0	0	0	0
3	0	0	0.7078	0	0.5095	0	0	0	0	0
4	0	-0.1855	0	0.5095	0	0.5336	0	0	0	0
5	0	0	0	0	0.5336	0	0.5358	0	-0.0724	0
6					0	0.5358	0	0.6343	0	0
7					0	0	0.6343	0	0.8127	0
8					0	-0.0724	0	0.8127	0	0.9871
L					0	0	0	0	0.9871	0

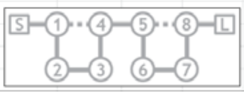

Figure 3: The synthesized coupling matrix, with the filter topology inset.

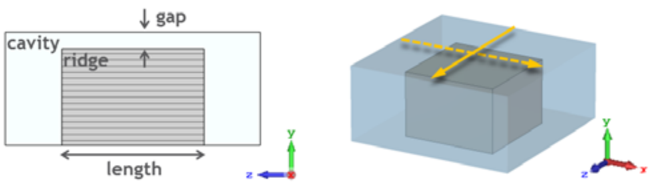

Figure 4: Ridged waveguide resonator, showing the cross-section (left) and 3D (right) view. Arrows show modal current directions.

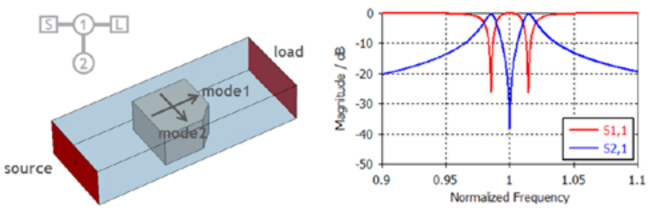

Figure 5: A single ridged resonator placed in a rectangular waveguide excited with the fundamental TE10 mode (left) and response (right).

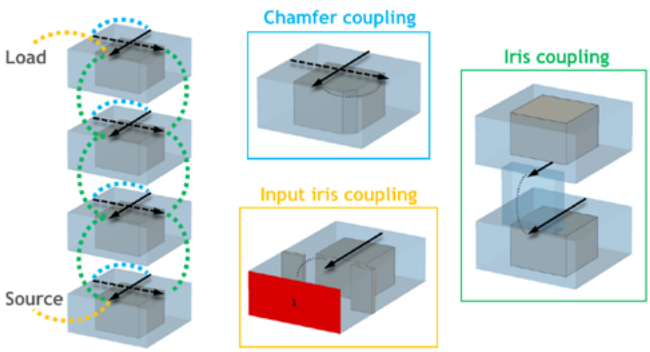

Figure 6: The proposed filter configuration, with an illustration of all the different coupling mechanisms.

RESONATOR DESIGN

In order to produce a compact device, a ridged waveguide dualmode resonator introduced by Bastioli[5] is used for the filter design. This resonator uses a rectangular waveguide with a large square ridge inside as shown in Figure 4. Two orthogonal quasi-transverse (TEM) modes can exist in the narrow gap between the ridge and the top wall, approximating a parallel plate. This means that the size of the gap and length of the ridge directly determines the resonant frequency of these modes and the stopband separating the next higher-order mode. For resonance at 10 GHz in a WR-90 waveguide, the ridge length is 12.76 mm for a chosen gap of 1.5 mm.

If this ridge is positioned at the transversal centre of a straight waveguide, the fundamental TE10 mode will only excite the longitudinally-directed mode ("mode 1"). A chamfered corner that perturbs the ridge symmetry causes the longitudinal mode to also couple into the transversal mode ("mode 2"), producing a dual band response with a transmission zero at the center frequency as shown in Figure 5.

COUPLING

Although it is possible to couple the resonators with simple H-plane irises, this adds complexity to later stages of the design process. The cavities have to be placed alongside one another, resulting in a bulky device and worse, the irises will sustain coupling between modal pairs. This means for example that there will be an unwanted coupling between modes 3 and 6 in the filter topology shown in Figure 3.

As an alternative, the resonators can be coupled by irises in the E-plane (i.e. at the broadside walls), with a separate iris for each pair of aligned modes. This offers more control over the couplings and allows the resonators to be stacked in a compact layout. The source and load couple through conventional H-plane irises. The couplings are summarized in Figure 6. Each coupling is first designed in isolation, using the Eigenmode Solver (E-Solver) in CST Studio Suite.

The first magnetic coupling, serving coefficients m23 and m67, is established between the aligned modes where the ridge gaps face each other as shown in Fig. 7(a). Here the even and odd-mode current distributions are shown for this coupling system, where a magnetic wall is placed on the symmetry axis of the current distribution to ensure the calculation of only the appropriate eigenmodes[6]. For this coupling, the coupling bandwidth (CBW) can be controlled by the height of the iris. The unwanted coupling between orthogonal ridge modes can then be reduced in a second calculation without compromising CBW, by adjusting the other parameters of the iris (replacing the magnetic wall with an electric wall). Similarly, the magnetic coupling for m45 is obtained with such an iris.

The electric coupling shown in Fig. 7(b) produces the values for the cross-coupling coefficients m14 and m58. Here, a thin but wide capacitive iris is used and the CBW is controlled by the offset of the iris to the resonator wall.

The remaining couplings – m12, m34, m56 and m76 – are produced by the chamfering of the ridge. These chamfers need to be carefully positioned within the complete layout, in order to avoid phase cancellation which will negate the designed iris couplings. Thus, to avoid this, all the chamfers are orientated in the same direction. Furthermore, they are also placed on opposite sides to the coupling irises of coefficients m23, m14, m67 and m58 to minimize the effect on the broadside couplings.

TUNING OF THE COMPLETE 3D STRUCTURE

Once all these couplings are combined into one 3D model, the full filter can be simulated. Here, the Model Order Reduction (MOR) technique in the Frequency Domain Solver significantly accelerates the simulation. The S-parameter results are shown in Figure 8 – at this stage in the design process, the filter is detuned due to the loading effects of the different components that have been designed in isolation. The transmission zero pairs of the detuned response are asymmetric, indicating coupling between unintended modes.

Using Filter Designer 3D, the coupling matrix for the filter is extracted, as shown in Figure 9. This shows how each coupling coefficient deviates from the desired synthesized value, including the parasitic coupling coefficients (marked here with an inductor symbol).

The next step is to determine what the correct dimensions of the filter should be to compensate for the unwanted deviations in the extracted coupling matrix. The relationship between the geometry and the filter parameters (f_0, external Q-factor and CBW) are obtained from the various models simulated with the E-Solver. The coupling matrix reveals that some of the largest deviations are found in the diagonal coefficients, which means that the resonant frequencies are out. This is compensated for by changing the corresponding ridge lengths.

Simulating the updated model shows that this has improved the filter response and achieved some matching around the center frequency. The new extracted coupling matrix shows that the diagonal coefficients are indeed improved. Instead of continuing this iterative process, the build-in optimizer can be used for the electromagnetic model with the goal function set to the desired Filter Designer 3D project. The Trust Region Framework (TRF) algorithm is selected to do a local search over all 18 parameters and reduce the extracted coupling matrix errors. After about 61 optimization steps all the matrix errors are below 2.5% and the resulting S11 curves are shown in Figure 10.

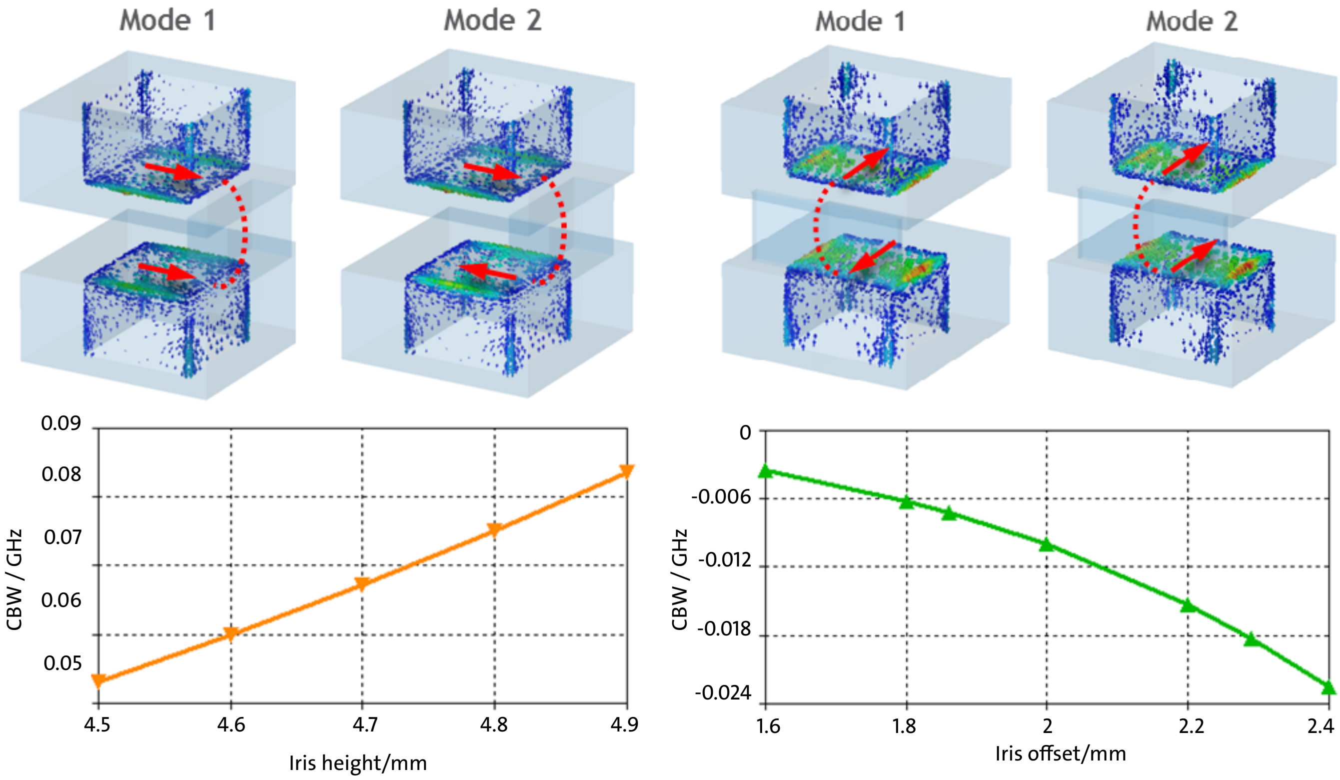

Figure 7: The current distributions of the (a) magnetic and (b) electric couplings established through the broadside irises. Each graph shows the dependency of the CBW on a corresponding geometrical parameter.

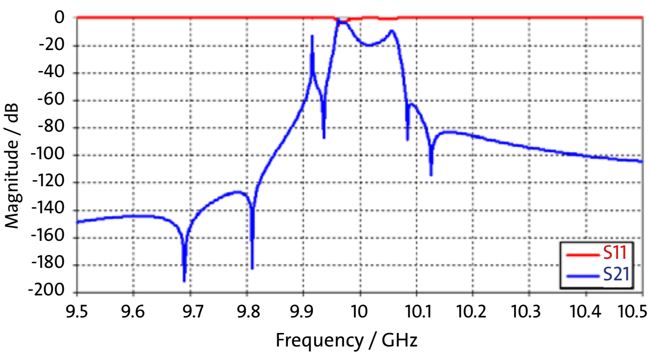

Figure 8: S-parameters for the untuned filter response.

	S	1	2	3	4	5	6	7	8	L
S	0.0	1.0005 +1.4%	0.0	0.0	0.0	0.0	0.0	0.0	0.0	0.0
1	1.0005 +1.4%	-0.68675 +34.3%	0.81287 +3.2%	0.043592 ≠ 0.0	-0.15763 -18.9%	0.0	0.0	0.0	0.0	0.0
2	0.0	0.81287 +3.2%	-0.081335 +7.9%	0.58114 -18.2%	0.043592 ≠ 0.0	0.0	0.0	0.0	0.0	0.0
3	0.0	0.043592 ≠ 0.0	0.58114 -18.2%	-0.69419 +39.9%	0.56612 +12.9%	0.0	0.0	0.0	0.0	0.0
4	0.0	-0.15763 -18.9%	0.043592 ≠ 0.0	0.56612 +12.9%	0.94475 -47.4%	0.54944 +3.1%	0.0	0.0	0.0	0.0
5	0.0	0.0	0.0	0.0	0.54944 +3.1%	1.0745 -53.7%	0.40752 -23.6%	0.054974 ≠ 0.0	-0.03001 -60.1%	0.0
6	0.0	0.0	0.0	0.0	0.0	0.40752 -23.6%	-0.75246 +34.3%	0.71819 +13.1%	0.054974 ≠ 0.0	0.0
7	0.0	0.0	0.0	0.0	0.0	0.054974 ≠ 0.0	0.71819 +13.1%	-0.16046 +5.3%	0.8127 +0.27%	0.0
8	0.0	0.0	0.0	0.0	0.0	-0.03001 -60.1%	0.054974 ≠ 0.0	0.8127 +0.27%	-0.54329 +27.1%	1.0005 +1.4%
L	0.0	0.0	0.0	0.0	0.0	0.0	0.0	0.0	1.0005 +1.4%	0.0

Figure 9: Coupling matrix of the initial filter response, showing the deviation from the specifications.

Because the filter is narrowband, the model is very sensitive. This makes it susceptible to mesh noise – the inherent inaccuracy caused by remeshing the structure, common to the Finite Element Method (FEM). In order to achieve the exacting specifications required, the Moving Mesh technique in CST Studio Suite is used. Rather than remeshing the structure for each optimization step, the software snaps the previous mesh to the new structure. This significantly reduces the mesh noise, allowing the optimizer to achieve the goal function.

The parameter space of the model is adjusted and the optimizer is executed to fine-tune the model to an equiripple passband as indicated by the final S-parameters in Figure 11. The transmission zeros are located asymmetrically around the passband, causing a steeper cut-off at the upper side while compromising the cut-off on the lower side. This effect is caused by the parasitic couplings in the structure which are difficult to fully control. Forcing symmetry on the transmission zero positions would again jeopardize the equiripple passband response and therefore causes a trade-off in performance. The overall size of the simulation model is 23 x 29 x 60 mm^3.

CONCLUSION

This article has demonstrated a complete workflow for the design of a compact ridged waveguide filter, all within CST Studio Suite. The Filter Designer 3D solver was used to select the filter topology and synthesize the coupling matrix, the Eigenmode Solver was used to design the individual resonators and couplings, and the Frequency Domain Solver with MOR was used to design the complete structure. Optimization using the Trust Region Framework and the Moving Mesh technique was used to fine-tune the filter and achieve excellent filter performance, producing a highly-sensitive filter with 1% FBW.

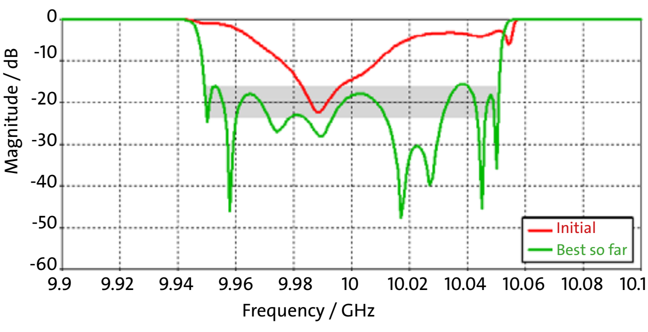

Figure 10: S11 of the 3D filter, after adjusting only the ridge lengths ("Initial") and then running the TRF optimization based on the extracted coupling matrix ("Best so far").

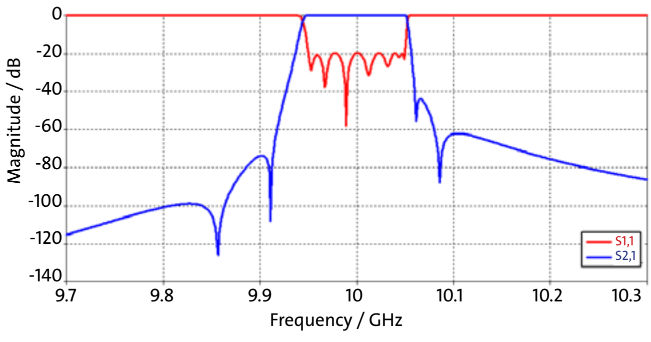

Figure 11: S-parameters of the filter response after optimization.

REFERENCES

[1] A. E. Atia and A. E. Williams, "New types of waveguide bandpass filters for satellite transponders," in COMSAT Technical Review, vol. 1, no. 1, 1971.

[2] F. Hirtenfelder, "Tuning methods for bandpass filters using CST STUDIO SUITE solver technology," in 4th CST European User Group Meeting, 2009.

[3] J. B. Ness, "A unified approach to the design, measurement, and tuning of coupled-resonator filters," IEEE Transactions on Microwave Theory and Techniques, vol. 46, no. 4, pp. 343–351, Apr 1998.

[4] Q. S. Cheng, J. C. Rautio, J. W. Bandler, and S. Koziel, "Progress in simulator-based tuning – the art of tuning space mapping," IEEE Microwave Magazine, vol. 11, no. 4, pp. 96–110, Jun 2010.

[5] L. M. S. Bastioli and R. Sorrentino, "A novel class of compact dualmode rectangular waveguide filters using square ridge resonators," in 38th European Microwave Conference (EuMC), 2008, pp. 626–629.

[6] CST Studio Suite, https://www.3ds.com/products-services/simulia/products/cst-studio-suite/

[7] S. Ratnajeevan, H. Hoole, K. Weeber, and S. Subramaniam, "Fictitious minima of object functions, finite element meshes, and edge elements in electromagnetic device synthesis," IEEE Transactions on Magnetics, vol. 27, no. 6, pp. 5214–5216, Nov 1991.

AUTHOR

Theunis S. Beukman, SIMULIA Solution Consultant Specialist

Americas
Dassault Systèmes
175 Wyman Street
Waltham, Massachusetts
02451-1223
USA

Europe/Middle East/Africa
Dassault Systèmes
10, rue Marcel Dassault
CS 40501
78946 Vélizy-Villacoublay Cedex
France

Asia-Pacific
Dassault Systèmes K.K.
ThinkPark Tower
2-1-1 Osaki, Shinagawa-ku,
Tokyo 141-6020
Japan